euspen's 23rd International Conference & Exhibition, Copenhagen, DK, June 2023
www.euspen.eu

Investigation of laser scanning parameters on the geometry of laser ablated hollow microneedle cavities

Tim Evens[1], Pol Vanwersch[1,2], Sylvie Castagne[2], Albert Van Bael[1]

[1] *KU Leuven, Department of Materials Engineering, Diepenbeek Campus, Belgium*
[2] *KU Leuven, Department of Mechanical Engineering and Flanders Make @KU Leuven-MaPS, Belgium*

Corresponding author: tim.evens@kuleuven.be

Abstract
Recently, a novel method to produce hollow polymer microneedles using laser ablated microneedle cavities in an injection moulding process has been developed. These ablated cavities are created using a femtosecond laser ablation process with a cross-hatching strategy. Various laser scanning parameters have an effect on the geometry of the microneedle cavities, which in turn have an influence on the functionality of the replicated needles. It is therefore key to understand how the laser scanning parameters affect the geometry of the microneedle cavities. In this work, three laser scanning parameters are varied, being the diameter of the scan-free area, the position of the scan-free area, and the number of layers. The geometry of the microneedle cavities is characterised using micro-computed tomography and a correlation between the laser scanning parameters and the shape of the microneedle cavity is provided. It is found that a higher number of layers increases the cavity diameter at the mould surface, increases the depth of the cavity and the ridge-forming trench, and decreases the diameter of the lumen-forming pillar. An increase in the eccentricity of the scan-free area increases the cavity depth and decreases the depth of the ridge-forming trench, while the depth of the lumen-forming pillar decreases sightly with an increase in the eccentricity of the scan-free area. All cavities created with a sufficiently large scan-free area have a lumen-forming pillar with the top being in plane with the mould surface, while the top of the lumen-forming pillar of cavities created with a smaller scan-free area are mostly located below the mould surface.

Microneedles; Micro manufacturing; Laser machining.

1. Introduction

Hollow microneedles are needle-like microscopic structures which can be used to pierce the skin [1]. These needles have a lumen, or internal bore, which enables the transportation of fluids to either deliver medical substances, or to extract fluids for sampling purposes. They are most often arranged in an array, having various shapes and lengths ranging from 25 to 2000 µm [2]. Recently, a novel method was developed to produce hollow polymer microneedles [3]. In this method, microneedle cavities with an internal lumen-forming pillar are created using a laser ablation process, and are afterwards replicated using polymer injection moulding. Various laser scanning parameters have an effect on the geometry of the microneedle cavities, which in turn affect the functionality of the replicated needles. Therefore, this work investigates the effect of three laser scanning parameters, being the diameter of the scan-free area, the position of the scan-free area, and the number of layers, on the geometry of the laser ablated microneedle cavities.

2. Material and methods

2.1. Material

The selected mould material is a low corrosion tool steel "Stavax" (grade 1.2083 - AISI 420), which is a common mould material for polymer injection moulding.

2.2. Laser machining experiments

A micromachining system (Lasea, Belgium) with a Satsuma HP femtosecond laser source (Amplitude, France) is employed for the laser ablation process. The laser source emits a beam with a pulse duration of 250 fs, a wavelength of 1030 nm and a pulse repetition rate of 500 kHz. The maximum average power of the laser on target is 7.85 W, giving a deliverable pulse energy of 15.7 µJ. The laser beam has a spot size of 15.0 µm diameter and an average pulse fluence of 8.88 J/cm².

A cross-hatching laser scanning strategy is used in this study for the creation of the hollow microneedle cavities and is illustrated in Figure 1 [3]. In this strategy, the laser spot scans a circular region, defined with a scanning diameter, and follows parallel lines in two perpendicular directions, where the distance between two consecutive lines is defined as the hatch pitch. Within the scanning diameter, a scan-free internal area with a specific position and diameter is defined to create the lumen-forming pillar inside the microneedle cavity. Once the laser has scanned one layer, the focal point is lowered with a vertical distance, defined as the layer pitch, and the laser scans again the same area. This process is repeated multiple times for a prescribed number of layers.

A design of experiments was formulated to identify the effect of different laser scanning parameters on the geometry of the microneedle cavity. The scanning parameters varied in this study are the number of layers, the diameter of the scan-free area, and the position of the scan-free area. The levels of the scanning parameters were identified based on experience gained throughout preliminary experiments. The number of layers was varied in three levels, being 150, 300, and 450. The diameter of the scan-free area was varied in two levels, being 100 µm and 150 µm. The position of the scan-free area, defined as the distance between the centre of the circular scanning region and the centre of the scan-free area, is varied in three levels being 75 µm, 100 µm, and 125 µm. This results in a total of 18 different

sets of laser scanning parameters. The scanning diameter, the hatch pitch, the layer pitch, and the scanning speed were fixed throughout all experiments at 500 µm, 15 µm, 2 µm, and 100 mm/s respectively.

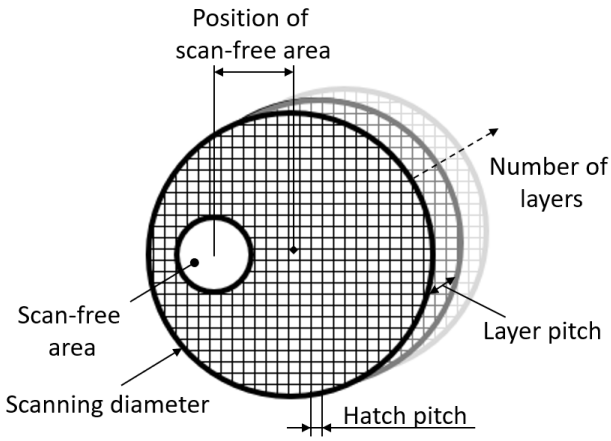

Figure 1. Illustration of the laser strategy with internal scan-free area.

2.3. Topography characterization

The geometries of the ablated microneedle cavities were characterized using a Phoenix Nanotom µ-CT system (Universal Systems, Solon, USA). The device is equipped with a high-power nanofocus X-ray tube and a diamond-tungsten target was chosen for the high X-ray absorbing steel samples. A high-power mode was used to allow focal spot and voxel sizes in the micrometre range. For each scan, 2400 X-ray 2D projection images were obtained from incremental rotation of the scanned samples over 360°. Acquisition parameters were fixed for all samples as follows: voltage = 140 kV, current = 50 µA, voxel size = 4 µm, and a 0.1 mm copper and 0.1 mm aluminium filter were used during scanning. Reconstruction of the acquired 2D projections into 3D volumes was performed using GE Phoenix datos|x REC software. Reconstructed datasets (slices) were exported from the software for further analysis and visualization within Fiji ImageJ. For each microneedle cavity, the depth of the cavity, depth of the ridge-forming trench, and depth of the lumen-forming pillar were measured (see Figure 2).

The cavity base diameter and the diameter of the lumen-forming pillar at the surface of the mould insert were measured using a Keyence VHX-500 digital microscope (Keyence, Osaka, Japan).

3. Results

3.1. Terminology for the geometric characteristics of the microneedle and microcavity

To understand the terminology that is used throughout this work, an illustration of the geometrical characteristics of a microneedle cavity and the corresponding replicated polycarbonate microneedle is provided in Figure 2. The microneedle cavity was created using following laser scanning parameters: 300 layers, a scan-free diameter of 100 µm, and a scan-free position of 125 µm.

The needle length and ridge height of the microneedle correspond to the replication of the cavity depth and ridge-forming trench, respectively. It is possible to improve the replication fidelity by adapting the injection moulding parameters, but this is beyond the scope of this work [4]. The function of this ridge is to prevent fluids from leaking between the microneedle and the skin of the patient when the microneedle is not fully inserted into the skin. It is therefore desired to have a high ridge. Another important characteristic of the microneedle cavity is the depth of the lumen-forming pillar, that will form the lumen of the microneedle when replicated. It is desired that the top of this pillar is in plane with the mould surface or, in other words, that the depth of the lumen-forming pillar is equal to zero. As such, the lumen will run through the full depth of the polymer microneedle.

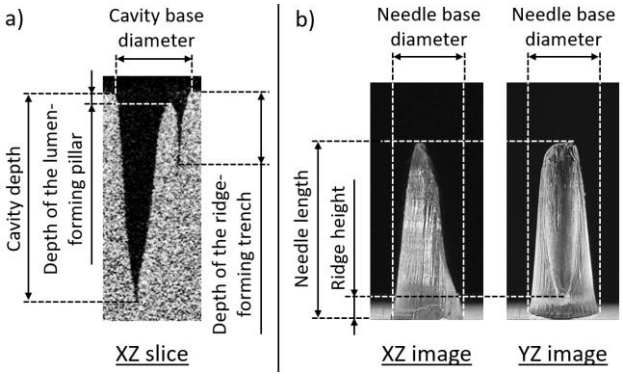

Figure 2. Illustration of the geometrical characteristics for: (a) an XZ slice of the microneedle cavity created with 300 layers, a scan-free diameter of 100 µm, and a scan-free position of 125 µm; (b) an XZ and XY microscopy image of the corresponding replicated microneedle in polycarbonate.

3.2. Cross sectional views of the microneedle cavities

Figure 3 depicts the cross sectional views obtained from the µ-CT measurements of the microneedle cavities created with the design of experiments for a scan-free area diameter of (a) 100 µm and (b) 150 µm. Cone-shaped hollow microneedle cavities with very small tip radii (a few micrometres) are observed for all sets of laser parameters. However, the shape and dimensions vary between the different microneedle cavities. The effect of the laser scanning parameters on the shape and dimensions of the microneedles will be discussed in more detail throughout the following sections.

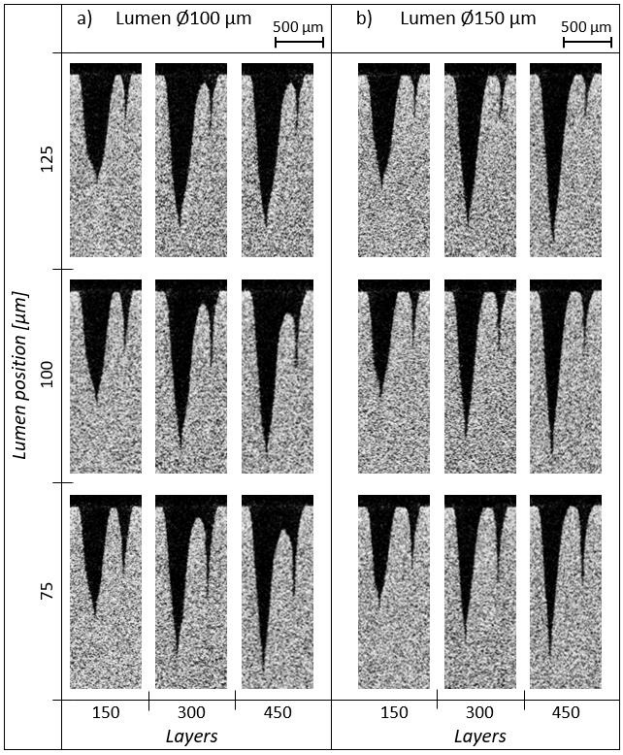

Figure 3. Cross sectional views obtained from the µ-CT measurements of the microneedle cavities created with the design of experiments for a scan-free area diameter of (a) 100 µm and (b) 150 µm.

3.3. Effect of the number of layers on the geometry of the microneedle cavity

Figure 4 displays the effect of the number of layers for a scan-free area diameter of 100 µm and 150 µm on the (a) cavity base diameter, (b) depth of the cavity and the ridge-forming trench, and (c) depth of the lumen-forming pillar, respectively. Each datapoint represents the average value over the different scan-free area positions.

3.3.1. Cavity base diameter

From Figure 4 (a), it is clear that the cavity diameter at the mould surface increases with a higher number of layers. Due to the programmed layer pitch, the focal spot is lowered with every layer. Therefore, the Gaussian shaped laser beam is defocused on the mould surface and it will start to interact with the edge of the already created microcavity. If the power density on the mould surface is higher than the ablation threshold, additional material will be removed. As such, a higher number of layers results in a larger cavity base diameter. Besides, it can be observed that the cavity base diameter is nearly identical for the scan-free area diameter of 100 µm and 150 µm. Thus, the diameter of the scan-free area has no effect on the cavity base diameter.

3.3.2. Depth of the cavity and the ridge-forming trench

In Figure 4 (b), it can be observed that the cavity depth increases with an increase in the number of layers for both the scan-free area diameter of 100 µm and 150 µm. This can easily be explained by the increase of accumulated fluence over the increased number of layers. However, the increase in depth slows down with higher numbers of layers. This trend is also observed for the ridge-forming trench created with a scan-free area diameter of 100 µm. In other words, there is a saturation in the depth after a certain number of layers. This was also observed in a previous work, in which the cavity depth of solid microneedle cavities was evaluated in function of the number of layers [6]. Within the present laser strategy, the saturation can be explained as follows: as an ablated hole gets deeper, the aspect ratio increases and the cavity walls become steeper. Therefore, the energy delivered to the target material is distributed over a larger area, resulting in a lower fluence. This, combined with an increase of the reflectivity on the steep walls, causes a drop in the ablation depth. The smaller the initial scanning area, the faster this saturation occurs. Hence, this also explains why the ridge-forming trench for the microneedle cavities with a scan-free area 150 µm is only increased slightly in function of the number of layers.

3.3.3. Depth of the lumen-forming pillar

In Figure 4 (c), it is observed that the depth of the lumen-forming pillar, created with a scan-free area diameter of 100 µm, increases with an increase in the number of layers. Yet, for all of the cavities created with a scan-free area diameter of 150 µm we observe that the top of the pillar is in plane with the mould surface. However, the surface area of the lumen-forming pillar at the mould surface also decreases in function of the number of layers. Similar to the explanation given in section 3.3.1., the Gaussian shaped laser beam will in this situation increasingly interacts with the edge of the lumen-forming pillar with an increase in the number of layers. Thus, the diameter of the top of the lumen-forming pillar is gradually decreased with an increase in the number of layers, until the top of the lumen-forming pillar is completely removed from the mould surface. At that point, the depth of the lumen-forming pillar will gradually increase.

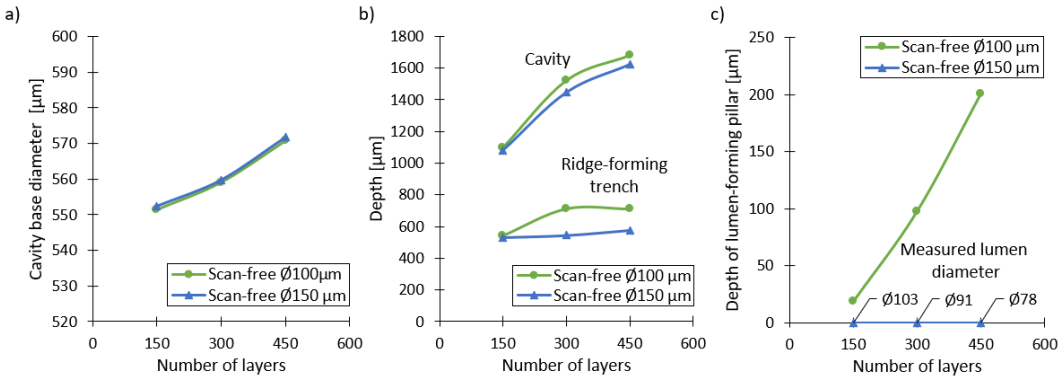

Figure 4. The effect of the number of layers for a scan-free area diameter of 100 µm and 150 µm is plotted for the (a) cavity base diameter, (b) depth of the cavity and the ridge-forming trench, and (c) depth of the lumen-forming pillar. Each datapoint represents the average value over the different positions of the scan-free area.

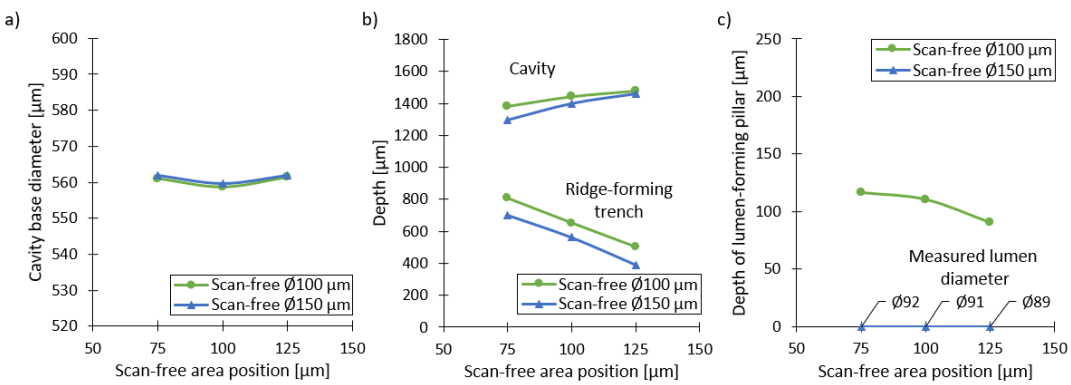

Figure 5. The effect of the scan-free area position for a scan-free area diameter of 100 µm and 150 µm is plotted for the (a) cavity base diameter, (b) depth of the cavity and the ridge-forming trench, and (c) depth of the lumen-forming pillar. Each datapoint represents the average value over the different number of layers.

3.4. Effect of the scan-free area position on the geometry of the microneedle cavity

Figure 5 displays the effect of the scan-free area position for a scan-free area diameter of 100 µm and 150 µm on the (a) cavity base diameter, (b) depth of the cavity and the ridge-forming trench, and (c) depth of the lumen-forming pillar, respectively. Each datapoint represents the average value over the different number of layers.

3.4.1. Cavity base diameter

Figure 5 (a) displays the cavity base diameter in function of the scan-free area position. It can be observed that the average diameter of the cavity (obtained for different number of layers) remains constant over the different scan-free area positions for both the scan-free area diameter of 100 µm and 150 µm. Thus, it can be concluded that the scan-free area position has no effect on the diameter of the microneedle cavity.

3.4.2. Depth of the cavity and the ridge-forming trench

Clear trends are observed between the scan-free area position and the depth of the cavity and the depth of the ridge-forming trench, as illustrated in Figure 5 (b). For both scan-free area diameters, an increase in the eccentricity of the scan-free area results in an increase in the cavity depth and a decrease in the depth of the ridge-forming trench. When the eccentricity of the scan-free area is increased, the surface area between the centre of the scanning diameter and the scan-free area is increased. In contrast, the scanning area between the scan-free area and the edge of the scanning diameter, which will form the ridge, is decreased. As already explained in section 3.3.2., the larger the available scanning area, the deeper the ablated cavity. As such, with an increase in the eccentricity of the scan-free area, the scanning area of the cavity increases while the scanning area of the ridge-forming trench decreases, resulting in an increase in the cavity depth and a decrease in the depth of the ridge-forming trench. This also explains why the depth of the ridge-forming trench for the cavity created with a scan-free area diameter of 150 µm is lower compared to the cavity with a programmed diameter of 100 µm.

3.4.3. Depth of the lumen-forming pillar

As already explained in section 3.3.3., it can be seen in Figure 5 (c) that all cavities created with a scan-free area diameter of 150 µm have a lumen-forming pillar with the top being in plane with the mould surface. Moreover, it can be observed that the diameter of those lumen-forming pillars at the mould surface remains nearly constant over the different scan-free area positions. However, for the microneedle cavities created with a diameter of 100 µm it is observed that the top of most of the lumen-forming pillars are located below the mould surface. In fact, the depth of the pillar decreases sightly in function of the position of the scan-free area. A possible explanation for this is that a higher eccentricity of the scan-free area corresponds to a small scanning area between the scan-free area and the edge of the scanning diameter. This in turn, results in less material being removed on this side of the lumen-forming pillar. However, the edge of the lumen-forming pillar near the middle of the cavity is still being ablated by the intersecting Gaussian laser beam. When the eccentricity of the scan-free area is decreased, the scanning area between the lumen-forming pillar and the edge of the scanning diameter is increased, resulting in a higher material removal at this side of the lumen-forming pillar. At the same time, there is still a high amount of material removal on the edge of the lumen-forming pillar near the middle of the cavity. As such, material is removed from both sides of the lumen-forming pillar, resulting in a higher depth of the lumen-forming trench.

4. Conclusion

This work investigated the effect of three laser scanning parameters on the geometry of the laser ablated microneedle cavities. The diameter of the scan-free area, the position of the scan-free area, and the number of layers were varied in a design of experiments, which resulted in a total of 18 different sets of laser scanning parameters.

It was found that the cavity diameter at the mould surface increased with a higher number of layers, due to the laser beam intersecting with the edge of the microneedle cavity. Besides, an increase in the number of layers increased the depth of both the cavity and the ridge-forming trench, due to the increase in accumulated fluence. However, there is a saturation in the depth after a certain number of layers, which is reached faster for smaller scanning areas. In addition, a higher number of layers increases the depth and decreases the diameter of the lumen-forming pillar.

An increase in the eccentricity of the scan-free area was found to increase the cavity depth and decrease the depth of the ridge-forming trench. At last, it was found that the depth of the lumen-forming pillar decreased slightly with an increase in the eccentricity of the scan-free area.

All cavities created with a scan-free area diameter of 150 µm have a lumen-forming pillar in plane with the mould surface. However, for the microneedle cavities created with a scan-free area diameter of 100 µm it is observed that most of the lumen-forming pillar are located below the mould surface.

Thanks to this work, we better understand the effect of the investigated laser scanning parameters on the geometry of the hollow microneedle cavities, which will facilitate the design of an optimal hollow microneedle cavity in the future.

Funding and acknowledgements

This work was funded by the KU Leuven Interdisciplinary Network project IDN/20/011 MIRACLE: Autonomous microfluidic patch for plasmid-based vaccine, as well as the Fonds Wetenschappelijk Onderzoek (FWO)–Vlaanderen SBO S003923N project and SB fellowship 1S31022N.

The authors would like to thank Olivier Malek from Sirris (department of Precision Manufacturing) for the laser ablation of the microneedle cavities.

References

[1] Evens T, Malek O, Castagne S, Seveno D, Van Bael A. A novel method for producing solid polymer microneedles using laser ablated moulds in an injection moulding process. Manuf Lett 2020;**24**:29–32.

[2] Donnelly RF, Singh TRR, Woolfson AD. Microneedle-based drug delivery systems: Microfabrication, drug delivery, and safety. Drug Deliv 2010;**17**:187–207.

[3] Evens T, Van Hileghem L, Dal Dosso F, Lammertyn J, Malek O, Castagne S, et al. Producing Hollow Polymer Microneedles Using Laser Ablated Molds in an Injection Molding Process. J Micro Nano-Manufacturing 2021;**9**:1–9.

[4] Evens T, Castagne S, Seveno D, Van Bael A. Comparing the Replication Fidelity of Solid Microneedles Using Injection Compression Moulding and Conventional Injection Moulding. Micromachines 2022;**13**:1280.

[5] Chichkov BN, Momma C, Nolte S, Alvensleben F, Tünnermann A. Femtosecond, picosecond and nanosecond laser ablation of solids. Appl Phys A Mater Sci Process 1996;**63**:109–15.

[6] Evens T, Malek O, Castagne S, Seveno D, Van Bael A. Controlling the geometry of laser ablated microneedle cavities in different mould materials and assessing the replication fidelity within polymer injection moulding. J Manuf Process 2021;**62**:535–45.